Atmospheric Environment 101 (2015) 41–48

Contents lists available at ScienceDirect

Atmospheric Environment

journal homepage: www.elsevier.com/locate/atmosenv

On the evaluation of global sea-salt aerosol models at coastal/orographic sites

M. Spada [a, *], O. Jorba [a], C. Pérez García-Pando [b, c], Z. Janjic [d], J.M. Baldasano [a, e]

[a] Barcelona Supercomputing Center – Centro Nacional de Supercomputación, Barcelona, Spain
[b] NASA Goddard Institute for Space Studies, New York, USA
[c] Department of Applied Physics and Applied Math, Columbia University, New York, USA
[d] National Centers for Environmental Prediction, College Park, MD, USA
[e] Universitat Politècnica de Catalunya, Barcelona, Spain

HIGHLIGHTS

- Sea-salt global models are often compared to surface concentration climatologies.
- Models exhibit strong biases at several coastal stations.
- Mesoscale phenomena can significantly affect model behavior in coastal stations.
- High model resolution strongly improved annual concentration trends.
- Caution may be taken when comparing global models in coastal stations.

ARTICLE INFO

Article history:
Received 1 July 2014
Received in revised form
7 November 2014
Accepted 9 November 2014
Available online 11 November 2014

Keywords:
Sea-salt aerosol
Global model evaluation
University of Miami Network
Surface concentration measurements
Coastal sites
Orographic effects

ABSTRACT

Sea-salt aerosol global models are typically evaluated against concentration observations at coastal stations that are unaffected by local surf conditions and thus considered representative of open ocean conditions. Despite recent improvements in sea-salt source functions, studies still show significant model errors in specific regions. Using a multiscale model, we investigated the effect of high model resolution (0.1° × 0.1° vs. 1° × 1.4°) upon sea-salt patterns in four stations from the University of Miami Network: Baring Head, Chatam Island, and Invercargill in New Zealand, and Marion Island in the sub-antarctic Indian Ocean. Normalized biases improved from +63.7% to +3.3% and correlation increased from 0.52 to 0.84. The representation of sea/land interfaces, mesoscale circulations, and precipitation with the higher resolution model played a major role in the simulation of annual concentration trends. Our results recommend caution when comparing or constraining global models using surface concentration observations from coastal stations.

1. Introduction

Sea-salt is one of the largest contributors to the aerosol mass in the atmosphere, with uncertain annual emission estimates ranging from 0.3 Pg to 30 Pg (Lewis and Schwartz, 2004). Sea-salt affects the radiative fluxes directly by interacting with shortwave and longwave radiation (Haywood et al., 1999; Ma et al., 2008), and indirectly by acting as cloud condensation nuclei (CCN) (Pierce and Adams, 2006, 2009). Therefore, future increases or decreases of sea-salt due to changes in surface wind speed, atmospheric stability, precipitation, and sea-ice cover could result in positive or negative feedbacks on the climate system (Struthers et al., 2011).

Modeling studies have attempted to constrain the sea-salt aerosol life-cycle, specially focusing on the sea-salt source function, which represents the largest source of uncertainty (Gong, 2003; Mårtensson et al., 2003; Lewis and Schwartz, 2004; Clarke et al., 2006; Caffrey et al., 2006; Jaeglé et al., 2011; Fan and Toon, 2011; Gryhte et al., 2014; Partanen et al., 2014). Sea-salt source functions in global models are constrained and/or evaluated with aerosol optical depth (AOD) observations from satellites and Sun photometers, wind speed and surface concentration measurements

* Corresponding author. Earth Sciences Department, Barcelona Supercomputing Center (BSC-CNS), Edificio Nexus II, c/ Jordi Girona 29, 08034 Barcelona, Spain.
E-mail address: michele.spada@bsc.es (M. Spada).

http://dx.doi.org/10.1016/j.atmosenv.2014.11.019

Table 1
Observation sites considered in this work. Labels UNI-MIAMI, NIWA, and SWAS stand for University of Miami Network, National Institute of Water and Atmospheric Research, and South African Weather Service, respectively.

Station	Latitude	Longitude	Contributor	Observation years
Sea-salt surface mass concentration				
Baring Head	41.28° S	174.87° E	UNI-MIAMI	1987–1996
Chatam Island	43.92° S	176.50° W	UNI-MIAMI	1983–1996
Invercargill	46.43° S	168.35° E	UNI-MIAMI	1983–1996
Marion Island	46.92° S	37.75° E	UNI-MIAMI	1992–1996
Precipitation and wind				
Baring Head	41.28° S[a]	174.87° E[a]	NIWA	1980–2010
Chatam Island	43.92° S[a]	176.50° W[a]	NIWA	1980–2010
Invercargill	46.43° S[a]	168.35° E[a]	NIWA	1980–2010
Marion Island	46.90° S	37.85° E	SWAS	1980–2010

[a] Stands for average on multiple observation sites at the corresponding model gridcell.

from experimental campaigns (Quinn and Bates, 2005), and surface concentration climatologies at coastal stations from the University of Miami Network (UNI-MIAMI) (Savoie and Prospero, 1977). The UNI-MIAMI measurements represent the most comprehensive and used global climatological dataset of sea-salt surface concentration. Global model studies use a subset of the UNI-MIAMI coastal stations that are barely affected by local surf conditions (i.e. local production by breaking waves) and thus considered representative of open ocean conditions.

In a recent work, Jaeglé et al. (2011) showed that the discrepancy with observations of a model including a widely used source function based on a power law dependence on wind speed (Gong, 2003) was a strong function of SST. Using cruise observations to derive an empirical source function depending on both wind speed and SST, Jaeglé et al. (2011) obtained model bias reductions of nearly a factor of two for both cruise and station observations. Although the fitted parameters in the source function of Jaeglé et al. (2011) are model dependent, Tsigaridis et al. (2013) and Spada et al. (2013) recently tested the source function and found improved agreement with surface concentration observations in comparison to a number of other schemes. However, simulations remain affected with uncertainties up to a factor of 2 or more. For example, Spada et al. (2013) found positive systematic biases of a 100% or more in Baring Head, Chatam Island, Invercargill and Marion Island, regardless of the source function applied in a global model at $1^\circ \times 1.4^\circ$ resolution. Simulations included a variety of combined source functions including the schemes of Gong (2003), Monahan et al. (1986), Smith et al. (1993), Mårtensson et al. (2003), and Jaeglé et al. (2011). Similarly, Tsigaridis et al. (2013) found strong overestimations in these stations, with most of the simulated monthly mean concentrations greater than the measured climatological values plus one standard deviation. In Jaeglé et al. (2011) a positive bias of about 100% was found in Marion Island, while negative biases in Baring Head and Invercargill were more pronounced when using the SST-dependent source function. Regardless of the source function or global model used, the annual trend in

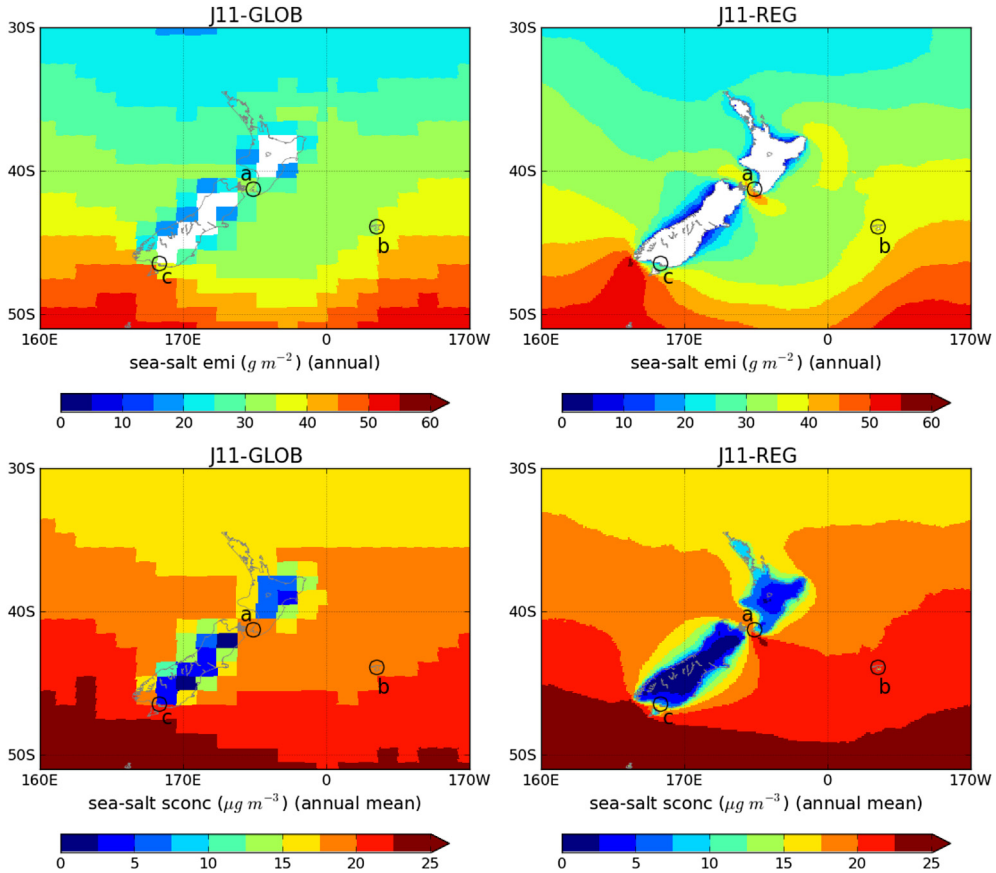

Fig. 1. Simulated sea-salt annual emission (upper panels) and annual mean surface concentration (bottom panels) at low (GLOB, left column) and high (REG, right column) model resolutions over New Zealand using the Jaeglé et al. (2011) (J11) source function. Simulated averages refer to a 5-year period (2002–2006). The labels emi and sconc refer to emission flux and surface concentration, respectively. Plots are displayed over zoomed regions with respect to simulated domains (covering latitudes from 148.8° E to 159.2° W and longitudes from 15.2° S to 67.2° S). *a*, *b*, and *c* indicate UNI-MIAMI stations (Baring Head, Chatam Island, and Invercargill, respectively).

Invercargill is not well captured (e.g. Liu et al. (2005); Jaeglé et al. (2011); Tsigaridis et al. (2013); Spada et al. (2013)).

Sea-salt emissions in the open ocean are relatively independent of model resolution compared to mineral dust emitted from arid regions (Ridley et al., 2013). However, some UNI-MIAMI coastal stations are surrounded by pronounced orographic gradients and/or complex sea/land interfaces (complex coastal areas and small islands). Therefore, even if free from surf-zone production, these stations may not be representative of open-ocean conditions from a meteorological point of view, which may affect the interpretation of global model evaluations. In this sense, we investigated the role played by model resolution in capturing topography, mesoscale circulations, and precipitation at these coastal/orographic regions, and how these aspects affected the sea-salt annual trends at the measurement stations. We focused on two regions including four UNI-MIAMI stations: the New Zealand region – including Baring Head (41.28° S, 174.87° E), Chatam Island (34.92° S, 176.50° W) and Invercargill (46.43° S, 168.35° E) – and Marion Island (46.92° S, 37.75° E).

2. Methodology

We used the multiscale NMMB/BSC Chemical Transport Model (Pérez et al., 2011; Haustein et al., 2012; Jorba et al., 2012) whose unified non-hydrostatic dynamical core allows for regional and global simulations (Janjic et al., 2011; Janjic and Gall, 2012). Sea-salt aerosol is represented by using a set of 8 size-bins ranging from 0.1 μm to 15 μm in dry radius. Details on the sea-salt aerosol module can be found in Spada et al. (2013). We compared global simulations at 1° × 1.4° horizontal resolution and 24 vertical levels (GLOB) with high-resolution regional simulations at 0.1° × 0.1° and 40 vertical levels. The global simulations and their evaluation were discussed in Spada et al. (2013). In this contribution, we considered two high-resolution regional domains (REG) centered in New Zealand (174.8° E, 41.2° S) and Marion Island (37.7° E, 46.1° S). For the global simulations we applied the source function of Gong (2003) (G03-GLOB) based on a power law dependence on wind speed and the source function of Jaeglé et al. (2011) (J11-GLOB) based on Gong (2003) with an added dependency on SST. For the regional simulations we used the source function of Jaeglé et al. (2011) (J11-REG). The dynamical core and all physical schemes were identical in both REG and GLOB simulations. The two REG domains were extended enough (i.e. more than 2000 km from the center of the domains, which represents five times the mean transport path of sea-salt aerosols at maximum wind speed conditions in the region) to avoid any noticeable sea-salt contribution from the boundaries of the domain to the study region. We performed 5-year simulations (2002–2006) in order to compare the model results with climatological observations. Simulations were initialized every 24 h and constrained at boundaries every 6 h with NCEP Final Analysis (FNL).

For the model evaluation we considered four stations from the UNI-MIAMI Network: (a) Baring Head, (b) Chatam Island, (c) Invercargill, and (d) Marion Island (see Table 1). Measurements are available from the early 1980s to the 1996 and these sites are free from surf-zone produced sea-salt aerosol (J. Prospero, personal communication, 2012). Observed sea-salt concentration was computed as $SS = Cl^- + 1.47Na^+$ (Quinn and Bates, 2005).

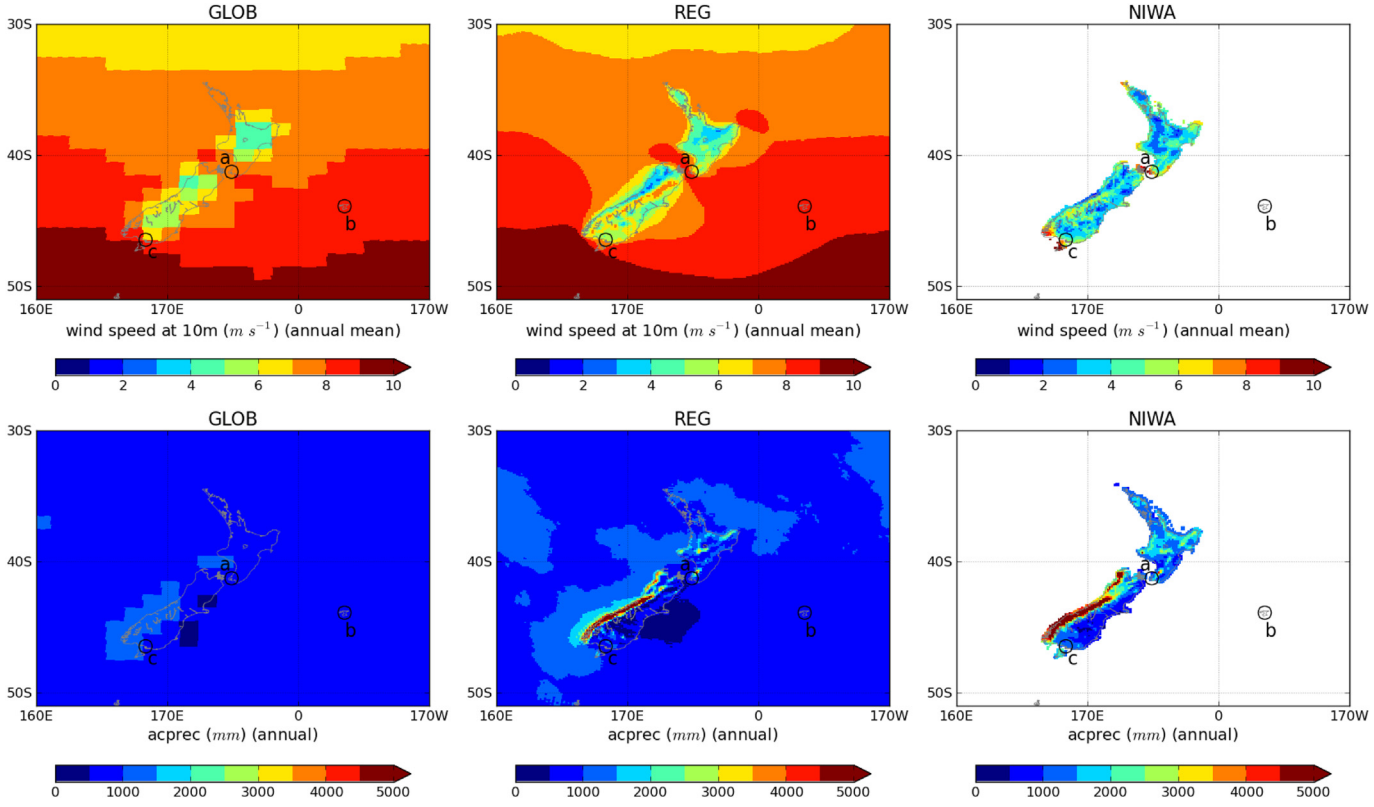

Fig. 2. Simulated annual mean wind speed at 10 m (upper panels) and annual accumulated precipitation (lower panels) at low (GLOB, left column) and high (REG, central column) model resolutions over New Zealand. 30-year observational climatologies from the National Institute of Water and Atmospheric Research (NIWA) are shown (right column). Simulated values cover a 5-year period (2002–2006). The label acprec refers to accumulated precipitation. Plots are displayed over zoomed regions with respect to simulated domains (covering latitudes from 148.8° E to 159.2° W and longitudes from 15.2° S to 67.2° S). *a*, *b*, and *c* indicate UNI-MIAMI stations (Baring Head, Chatam Island, and Invercargill, respectively).

Measurements are not constrained by an upper cutoff in radius. We also evaluated the simulated wind speed and precipitation with 30-year observational climatologies (1980–2010) provided by the National Institute of Water and Atmospheric Research (NIWA) (Wratt et al., 2006) and the South African Weather Service (SWAS) (Rouault et al., 2005) (Table 1). Additionally, NIWA provided climatological maps covering the New Zealand islands at $0.5^\circ \times 0.5^\circ$ resolution.

3. Results and discussion

The New Zealand region is characterized by open ocean westerlies and extratropical cyclones colliding with steep orographic gradients, which represent a classic example of the barrier problem (e.g. Roe (2005)). The influence of the Southern Alps orographic gradients upon wind and precipitation patterns represents a well studied topic both experimentally (Sinclair et al., 1997; McCauley and Sturman, 1999; Wratt et al., 2000) and through regional modeling (Katzfey, 1995a, b; Bormann and Marks, 1999; Revell et al., 2002). Westerlies have to circumvent the barrier and the flux is enhanced at the edges of the Island; rising humid air cools by adiabatic expansion releasing precipitation at the windward side of the mountain and becomes drier at the leeward side.

The Southern Alps are around 40 km wide and over 1.5 km high, with maximum heights of 3 km. Therefore, at REG scales (λ_{REG}) the model was able to capture the spatial length characterizing the orographic gradients $\lambda_c = 40$ km ($\lambda_c \sim 5\lambda_{REG}$) in contrast to GLOB ($\lambda_c/\lambda_{GLOB} < 1$). Fig. 1 shows the simulated annual sea-salt emission fluxes and annual mean surface concentration over the domain, both at low and high-resolution. At high-resolution (REG), the annual mean surface concentration decreased over New Zealand from 20% to 80% compared to the GLOB simulation. Marked changes in concentration patterns also were found in the New Zealand straits that neighbor Baring Head (a) and Invercargill (c), respectively. Furthermore, Chatam Island (b) was treated as a land grid cell with no direct emission in the REG simulation, while it was represented as an ocean grid cell in the GLOB simulation, leading to a decrease of roughly 30%.

Fig. 2 shows the simulated annual mean wind speed at 10 m and annual precipitation over the New Zealand domain compared to the NIWA climatological maps. Simulated and observed wind roses at Invercargill are also displayed in Fig. 3. Meteorological patterns changed significantly. At REG scales wind speed increased up to 20% compared to GLOB at the Cook Strait (between North and South Islands) and the edges of the Island. Over land, wind speed generally decreased, except for a narrow region leeward of the Southern Alps where winds increased up to 6–8 m/s, in better agreement with the observed NIWA climatology. Precipitation was enhanced to the west of the Island, including the open ocean and specially windward of the Southern Alps with a 800% increase. The maximum values and fine structure of precipitation were in strong agreement with the NIWA climatological map. Simulated precipitations upwind of the Southern Alps increased from 1200 mm/yr with GLOB to 10,300 mm/yr with REG, removing most of the bias with respect to the NIWA maximum values (around 11,200 mm/yr). The fine structure of the North Island and its local maxima were also well reproduced. The results outline the high-resolution model's ability to capture characteristic scales of the New Zealand circulation.

We also explored simulations over a large domain including Marion Island. Maps of sea-salt emission and surface concentration, wind speed at 10 m, and precipitation are displayed in Figs. 4 and 5. Marion Island (d) is a small volcanic island with steep orography (around 20 km of diameter and up to 1200 m altitude), subjected to strong northwesterly winds and high precipitation all year round. Regardless of the source function and global model, studies have shown systematic overestimations of the sea-salt surface concentration measured by the UNI-MIAMI station in this location. At the resolutions used by global models, the Island is considered as an open-ocean grid cell, and when REG scales were adopted, the sea/land interface was properly resolved by the model. In addition, precipitation was enhanced (up to 200% with respect to GLOB) windward of the orographic barrier. Consequently, an overall decrease of monthly mean concentrations from roughly 20 $\mu g/m^3$ (J11-GLOB) to 10 $\mu g/m^3$ (J11-REG) takes place over the Island.

Figs. 6 and 7 show the evaluation at the UNI-MIAMI measurement sites. The scatterplots indicate the significant improvement introduced when using high resolution. The strong positive bias affecting GLOB was reduced from +63% (J11-GLOB) to +3.3% (J11-REG) and the overall correlation increased from 0.52 to 0.84. The positive impact of model resolution was at least as large as the introduction of the SST-dependence in the G03 source function (bias reduced from +124% (GO3-GLOB) to +63% (J11-GLOB) and

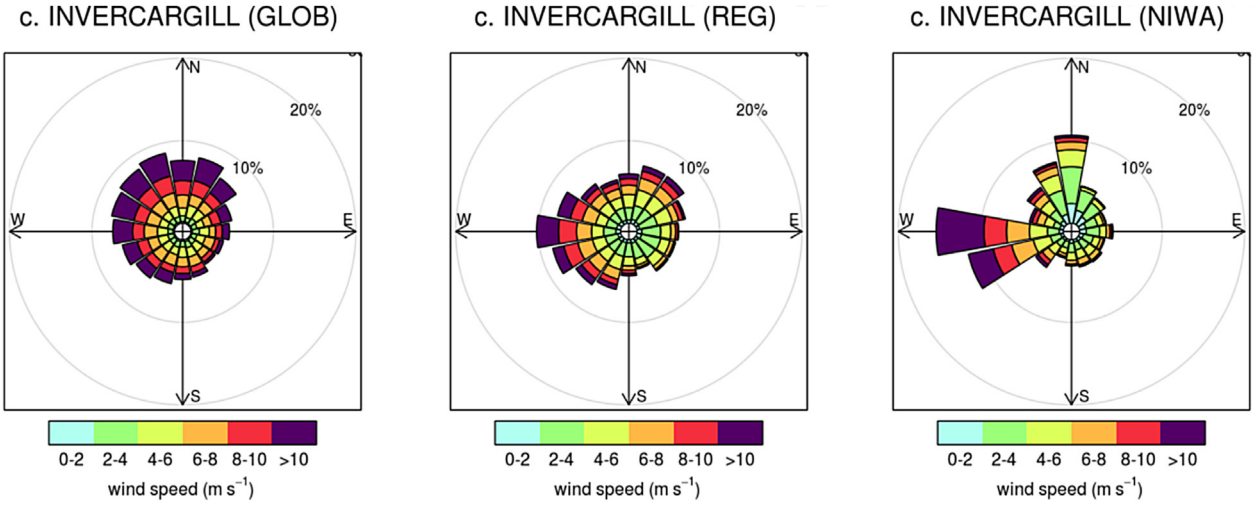

Fig. 3. Simulated wind rose of Invercargill (c) at low (GLOB, left panel) and high (REG, central panel) model resolutions over New Zealand. 30-year observational climatologies from the National Institute of Water and Atmospheric Research (NIWA) are shown (right panel). Simulated values cover a 5-year period (2002–2006).

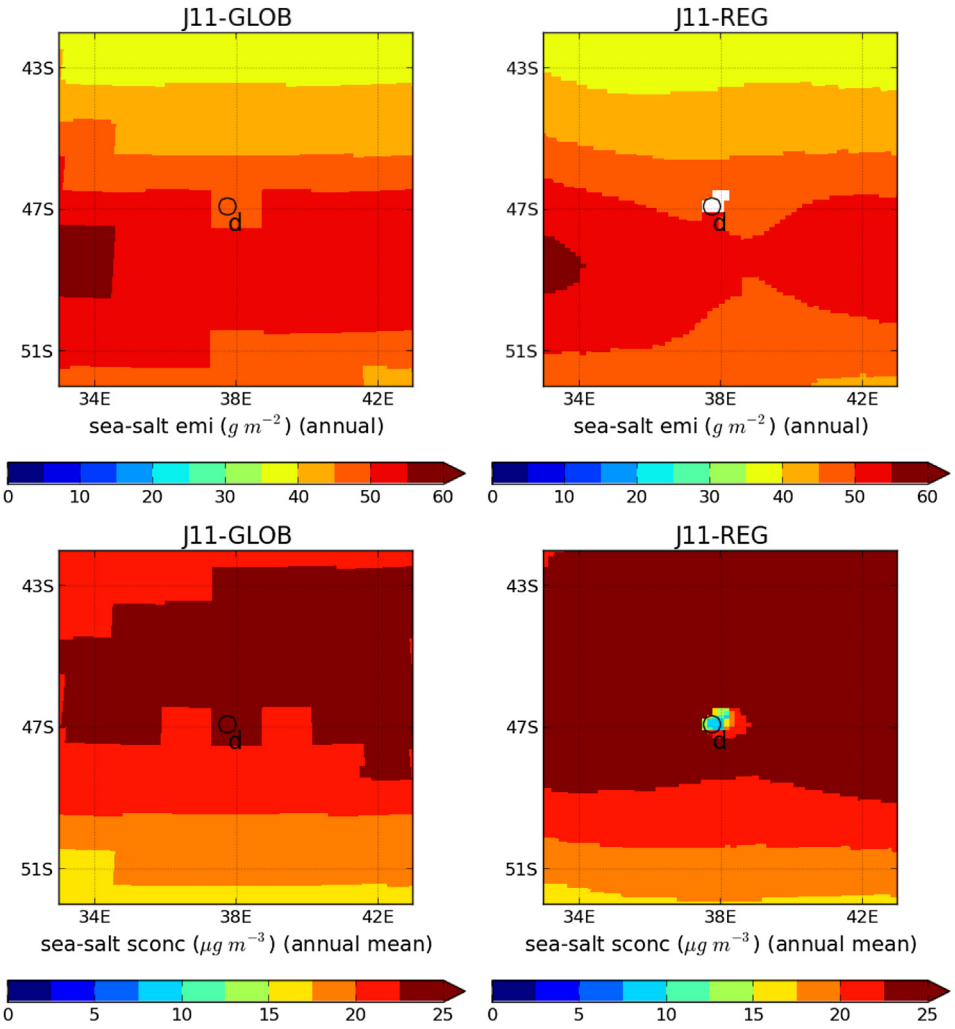

Fig. 4. Simulated sea-salt annual emission (upper panels) and annual mean surface concentration (bottom panels) at low (GLOB, left column) and high (REG, right column) model resolutions over Marion Island using the Jaeglé et al. (2011) (J11) source function. Simulated averages refer to a 5-year period (2002–2006). The labels emi and sconc refer to emission flux and surface concentration, respectively. Plots are displayed over zoomed regions with respect to simulated domains (covering latitudes from 12.7° E to 62.7° E and longitudes from 21.9° S to 71.9° S). *d* indicates the UNI-MIAMI Marion Island station.

correlation increased from 0.36 to 0.52), which makes evident that these effects may be taken into consideration when evaluating source functions at these sites. The positive bias of wind speed at 10 m was reduced from +24.6% to +15.8% and the correlation increased from 0.62 to 0.89. Remarkably, the high-resolution model was able to significantly reduce the overestimations of the wind speed monthly averages below 6 m/s. The simulation of precipitation improved with a reduction of the negative bias from −31.4% to −7.1%. In particular, the underestimated high monthly mean precipitations were corrected towards the observed values. The precipitation correlation increased from 0.65 to 0.86.

We identified three different effects introduced by the enhanced model resolution. When the model was able to properly solve small islands and represented them as land grid cells instead of ocean cells, sea-salt aerosol was not directly produced in such cells and the sea-salt surface concentration strongly decreased: this was mostly the case of Chatam Island (b). At Invercargill (c), the simulated wind circulation was strongly affected by the representation of the Southern Alps barrier. The model scales were able to capture the mesoscale circulation, with wind speed reductions and changes in wind direction in better agreement with the measured climatologies. Fig. 3 shows how the unrealistic wind rose at Inverncargill (c) with the GLOB simulations was clearly improved in the REG simulation, which better matched the observed dominant western winds and the lower wind speed values observed in other directions. Emissions and transport were consequently affected and the simulated surface concentrations decreased towards the observed monthly averages. We highlight the significant improvements introduced in the annual trend at Invercargill (c). The spurious maximum value in September obtained with GLOB simulations (also found in Liu et al. (2005) and Jaeglé et al. (2011)) was suppressed and replaced by a minimum value in August, in better agreement with the measured climatology. At Baring Head (a) and Marion Island (d) we observed a significant increase in simulated precipitation when high-resolution was used, in agreement with measurements, with subsequent enhancement of sea-salt wet-deposition (not shown) and a decrease in concentration. Being Baring Head (a), Invercargill (c) and Marion Island (d) stations located close to the coastal line, model results in these sites were also affected by the sea/land interface effect discussed for Chatam Island (b). The quantification of the relative importance of each of these effects is complex and beyond the scope of this contribution.

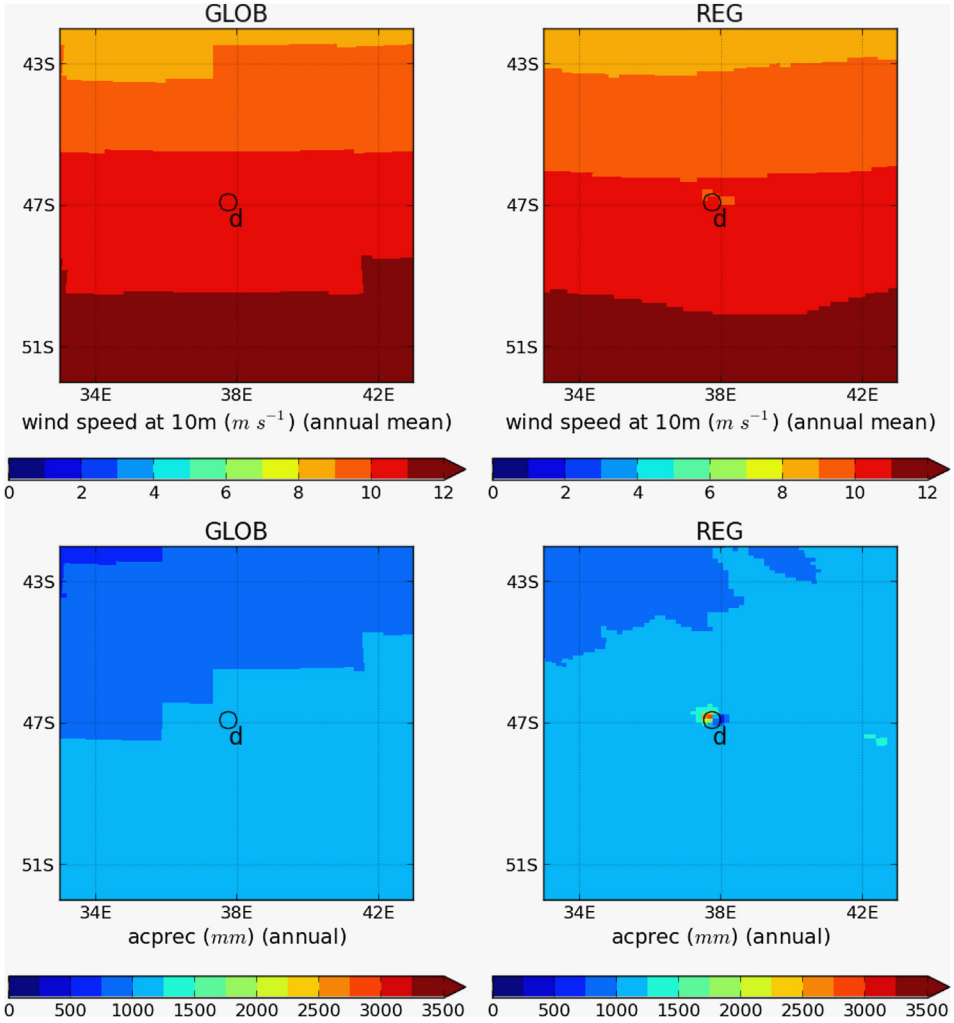

Fig. 5. Simulated annual mean wind speed at 10 m (upper panels) and annual accumulated precipitation (bottom panels) at low (GLOB, left column) and high (REG, right column) model resolutions over Marion Island. Simulated values cover a 5-year period (2002–2006). The label acprec refers to accumulated precipitation. Plots are displayed over zoomed regions with respect to simulated domains (covering latitudes from 12.7° E to 62.7° E and longitudes from 21.9° S to 71.9° S). *d* indicates the UNI-MIAMI Marion Island station.

4. Conclusions

We investigated the influence of model resolution on the simulation of sea-salt aerosol trends at global evaluation stations located in regions characterized by strong orographic gradients and/or complex sea/land interfaces. We selected four stations from the University of Miami Network where different global models presented significant errors when compared with sea-salt surface concentration climatologies. We showed that an increase of model resolution from 1° × 1.4° to 0.1° × 0.1° without changing any model scheme resulted in a strong bias reduction from +63.7% to 3.3% and an increase in the overall correlation from 0.52 to 0.84. The improvement of model results may be related to a better reproduction of sea/land interfaces and the characterization of mesoscale circulations and precipitation. We note that model experiments at 0.5° and 0.25° (not reported here) did not show

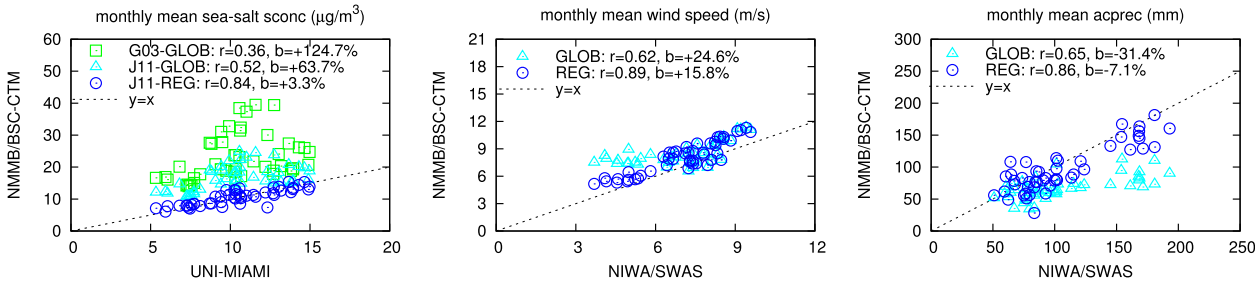

Fig. 6. From left to right: scatterplots of simulated versus observed monthly mean sea-salt surface concentrations (sconc), wind speed at 10 m, and precipitation (acprec); green squares, cyan triangles and blue circles refer to G03-GLOB (emission source of Gong (2003) at low resolution), J11-GLOB (emission source of Jaeglé et al. (2011) at low resolution), and J11-REG (emission source of Jaeglé et al. (2011) at high resolution) results, respectively. *r* and *b* stand for overall correlation and normalized bias. Simulated values cover a 5-year period (2002–2006). (For interpretation of the references to color in this figure legend, the reader is referred to the web version of this article.)

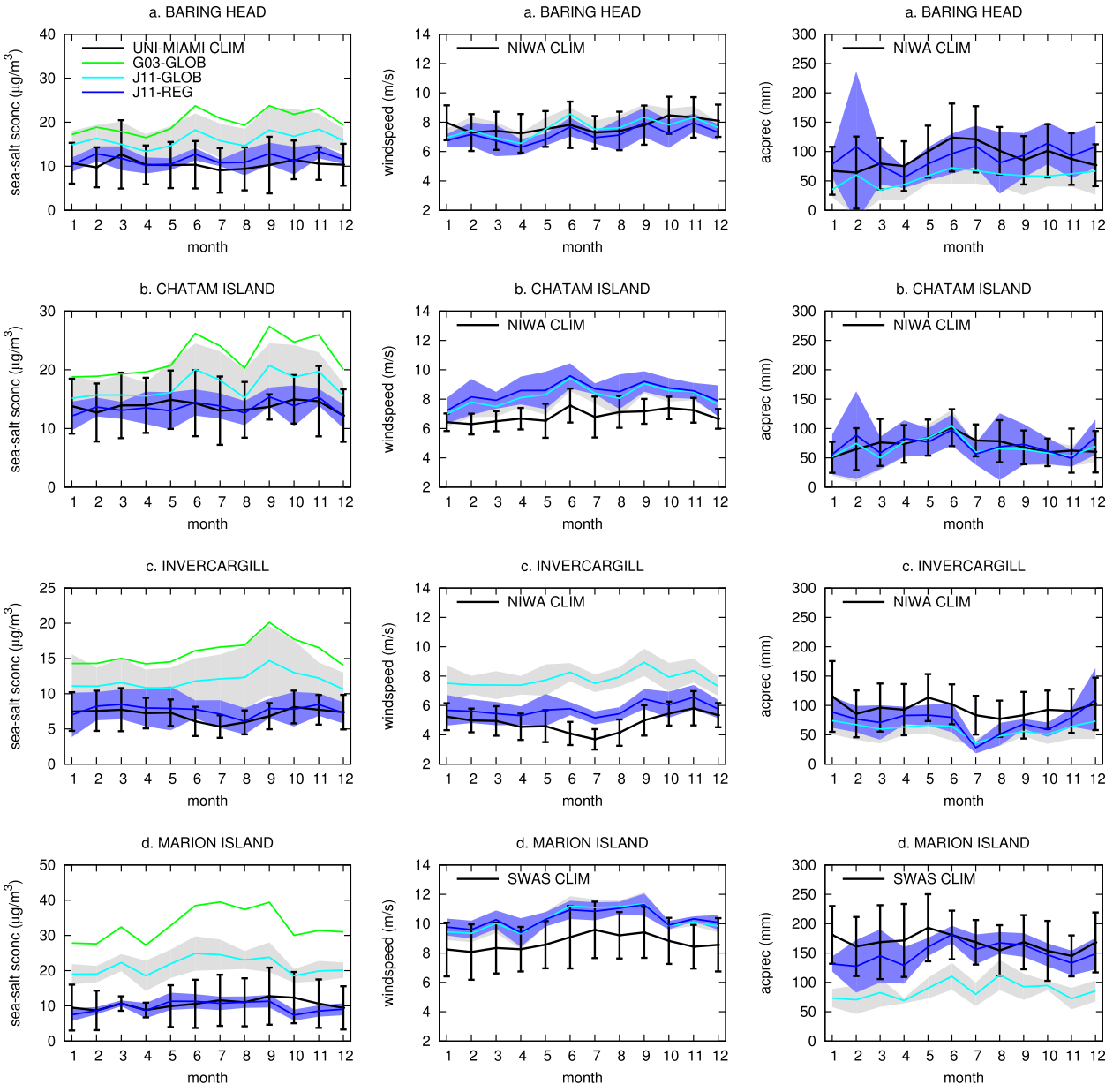

Fig. 7. Simulated and observed monthly mean values of surface concentration (left column), wind speed at 10 m (central column), and precipitation (right column) in each considered station; green, cyan, and blue lines refer to G03-GLOB, J11-GLOB, and J11-REG results, respectively. The label CLIM stands for climatologies. Observational climatologies (black lines, including standard error deviation bars) are from the University of Miami Network (UNI-MIAMI), the National Institute of Water and Atmospheric Research (NIWA), and the South African Weather Service (SWAS). Simulated values cover a 5-year period (2002–2006). J11-GLOB and J11-REG interannual standard deviation are also shown (shaded gray and blue, respectively). (For interpretation of the references to color in this figure legend, the reader is referred to the web version of this article.)

improvements with respect to the experiments at $1^\circ \times 1.4^\circ$. Resolutions of at least 0.1° are needed to reproduce the observations at these sites.

Our results suggest that caution may be taken when evaluating and/or constraining sea-salt global models with measurements from sites affected by coastal/orographic effects. Systematic errors in these sites due to the use of coarse resolution in global models can strongly affect the interpretation of model results that compare sea-salt source functions of the open ocean.

Acknowledgments

We would like to thank the scientists of the University of Miami Ocean Aerosol Network, the National Institute of Water and Atmospheric Research, and the South African Weather Service for establishing and providing data from the stations used in this work. In particular, we thank J. Prospero for his personal communications, M. Schulz for providing postprocessing of the University of Miami Ocean Aerosol Network dataset, and A. Tait for providing post-processing of the National Institute of Water and Atmospheric Research climatological maps. We also thank F. Benincasa for technical support. BSC acknowledges the support from projects CGL2013-46736-R and “Supercomputación and e-ciencia” Project (CSD2007-0050) from the Consolider-Ingenio 2010 program of the Spanish Ministry of Economy and Competitiveness and the support from the grant SEV-2011-00067 of Severo Ochoa Program, awarded by the Spanish Government. Carlos Pérez García-Pando acknowledges DoE and NASA Roses.

References

Bormann, N., Marks, C.J., 1999. Mesoscale rainfall forecasts over New Zealand during SALPEX96: characterization and sensitivity studies. Mon. Weather Rev. 127, 2880–2893.

Caffrey, P.F., Hoppel, W.A., Shi, J.J., 2006. A one-dimensional sectional aerosol model integrated with mesoscale meteorological data to study marine boundary layer aerosol dynamics. J. Geophys. Res. 111, D24201.

Clarke, A.D., Owens, S.R., Zhou, J., 2006. An ultrafine sea-salt flux from breaking waves: implications for cloud condensation nuclei in the remote marine atmosphere. J. Geophys. Res. 111, D06202.

Fan, T., Toon, O.B., 2011. Modeling sea-salt aerosol in a coupled climate and sectional microphysical model: mass, optical depth and number concentration. Atmos. Chem. Phys. 11, 4587–4610.

Gong, S.L., 2003. A parameterization of sea-salt aerosol source function for sub and super-micron particles. Glob. Biogeochem. Cycles 17, 1097.

Gryhte, H., Ström, J., Krejci, R., Quinn, P., Stohl, A., 2014. A review of sea-spray aerosol source functions using a large global set of sea salt aerosol concentration measurements. Atmos. Chem. Phys. 14, 1277–1297.

Haustein, K., Pérez, C., Baldasano, J.M., Jorba, O., Basart, S., Miller, R.L., Janjic, Z., Black, T., Nickovic, S., Todd, M.C., Washington, R., Müller, D., Tesche, M., Weinzierl, B., Esselborn, M., Schladitz, A., 2012. Atmospheric dust modeling from meso to global scales with the online NMMB/BSC-dust model – Part 2: experimental campaigns in Northern Africa. Atmos. Chem. Phys. 12, 2933–2958.

Haywood, J., Ramaswamy, V., Soden, B., 1999. Tropospheric aerosol climate forcing in clear sky satellite observation over the oceans. Science 283, 1299–1303.

Jaeglé, L., Quinn, P.K., Alexander, B., Lin, J.T., 2011. Gobal distribution of sea salt aerosols: new costraints from in situ and remote sensing observations. Atmos. Chem. Phys. 11, 3137–3157.

Janjic, Z.I., Gall, R., 2012. Scientific Documentation of the NCEP Nonhydrostatic Multiscale Model on the B Grid (NMMB). Part 1 Dynamics. Technical Report. NCAR/TN-489+STR.

Janjic, Z.I., Janjic, T., Vasic, R., 2011. A class of conservative fourth order advection schemes and impact of enhanced formal accuracy on extended range forecasts. Mon. Weather Rev. 139, 1556–1568.

Jorba, O., Dabdub, D., Blaszczak-Boxe, C., Pérez, C., Janjic, Z., Baldasano, J.M., Spada, M., Badia, A., Gonçalves, M., 2012. Potential significance of photoexcited NO_2 on global air quality with the NMMB/BSC chemical transport model. J. Geophys. Res. 117, D13301.

Katzfey, J.J., 1995a. Simulation of extreme New Zealand precipitation events. Part I. Sensitivity of orography and resolution. Mon. Weather Rev. 123, 737–754.

Katzfey, J.J., 1995b. Simulation of extreme New Zealand precipitation events. Part II. Mechanisms of precipitation development. Mon. Weather Rev. 123, 755–775.

Lewis, E.R., Schwartz, S.E., 2004. Sea Salt Aerosol Production: Mechanisms, Methods, Measurements, and Models. American Geophysical Union, Washington DC, pp. 9–13.

Liu, X., Penner, J.E., Herzog, M., 2005. Global modeling of aerosol dynamics: model description, evaluation, and interactions between sulfate and nonsulfate aerosols. J. Geophys. Res. 110, D18206.

Ma, X., von Salzen, K., Li, J., 2008. Modelling sea salt aerosol and its direct and indirect effects on climate. Atmos. Chem. Phys. 8, 1311–1327.

Mårtensson, E.M., Nilsson, E.D., de Leeuw, G., Cohen, L.H., Hansson, H.C., 2003. Laboratory simulations and parameterization of the primary marine aerosol production. J. Geophys. Res. 108, 4297.

McCauley, M.P., Sturman, A.P., 1999. A study of orographic blocking and barrier wind development upstream of the Southern Alps, New Zealand. Meteorol. Atmos. Phys. 70, 121–131.

Monahan, E.C., Spiel, D.E., Davidson, K.L., 1986. A model of marine aerosol generation via whitecaps and wave disruption. In: Monahan, E.C., Mac Niocaill, G. (Eds.), Oceanic Whitecaps. D. Reidel, Norwell, Massachusetts, pp. 167–174.

Partanen, A.I., Dunne, E.M., Bergman, T., Laakso, A., Kokkola, H., Ovadnevaite, J., Sogacheva, L., Baisnée, D., Sciare, J., Manders, A., O'Dowd, C., de Leeuw, J., Korhonen, H., 2014. Global modelling of direct and indirect effects of sea spray aerosol using a source function encapsulating wave state. Atmos. Chem. Phys. 14, 4537–4597.

Pérez, C., Haustein, K., Janjic, Z., Jorba, O., Huneeus, N., Baldasano, J.M., Black, T., Basart, S., Nickovic, S., Miller, R.L., Perlwitz, J., 2011. An online mineral dust aerosol model for meso to global scales: 1. Model description, annual simulations and validation. Atmos. Chem. Phys. Discuss. 11, 17551–17620.

Pierce, J.R., Adams, P.J., 2006. Global evaluation of CCN formation by direct emission of sea salt and growth of ultrafine sea salt. J. Geophys. Res. 11, D06203.

Pierce, J.R., Adams, P.J., 2009. Uncertainty in global CCN concentrations from uncertain aerosol nucleation and primary emission rates. Atmos. Chem. Phys. 9, 1339–1356.

Quinn, P.K., Bates, T.S., 2005. Regional aerosol properties: comparisons of boundary layer measurements from ACE1, ACE2, aerosols99, INDOEX,ACE asia, TARFOX, and NEAQS. J. Geophys. Res. 110, D14202.

Revell, M.J., Copeland, J.H., Larsen, H.R., Wratt, D.S., 2002. Barrier jets around the Southern Alps of New Zealand and their potential to enhance alpine rainfall. Atmos. Res. 61, 277–298.

Ridley, D.A., Heald, C.L., Pierce, J.R., Evans, M.J., 2013. Toward resolution-independent dust emissions in global models: impacts on the seasonal and spatial distribution of dust. Geophys. Res. Lett. 40, 2873–2877.

Roe, G.H., 2005. Orographic precipitation. Annu. Rev. Earth Planet. Sci. 33, 645–671.

Rouault, M., Mélice, J.L., Reason, C.J.C., Lutjeharms, T.R.E., 2005. Climate variability at Marion Island, southern ocean, since 1960. J. Geophys. Res. 110, C05007.

Savoie, D.L., Prospero, J.M., 1977. Aerosol concentration statistics for the Northern Tropical Atlantic. J. Geophys. Res. 82, 5954–5964.

Sinclair, M., Wratt, D.S., Henderson, R.D., Gray, W.R., 1997. Factors affecting the distribution and spillover of precipitation in the Southern Alps of New Zealand a case study. J. Appl. Meteorol. 36, 428–442.

Smith, M.H., Park, P.M., Consterdine, I.E., 1993. Marine aerosol concentrations and estimated fluxes over the sea. Q. J. R. Meteorol. Soc. 809–824.

Spada, M., Jorba, O., Pérez García-Pando, C., Janjic, Z., Baldasano, J.M., 2013. Modeling and evaluation of the global sea-salt aerosol distribution: sensitivity to size-resolved and sea-surface temperature dependent emission schemes. Atmos. Chem. Phys. 13, 11735–11755.

Struthers, H., Ekman, A.M.L., Glantz, P., Iversen, T., Kirkevåg, A., Mårtensson, E.M., Seland, Ø., Nilsson, E.D., 2011. The effect of sea ice loss on sea salt aerosol concentrations and the radiative balance in the Arctic. Atmos. Chem. Phys. 11, 3459–3477.

Tsigaridis, K., Koch, D., Menon, S., 2013. Uncertainties and importance of sea spray composition on aerosol direct and indirect effects. J. Geophys. Res. 118, 220–235.

Wratt, D.S., Revell, M.J., Sinclair, M.R., Gray, W.R., Henderson, R.D., Chater, A.M., 2000. Relationships between air mass properties and mesoscale rainfall in New Zealands Southern Alps. Atmos. Res. 52, 261–282.

Wratt, D.S., Tait, A., Griffiths, G., Espie, P., Jessen, M., Keys, J., Ladd, M., Lew, D., Lowther, N., Mitchell, N., Morton, J., Reid, J., Reid, S., Richardson, A., Sansom, J., Shankar, U., 2006. Climate for crops: integrating climate data with information about soils and crop requirements to reduce risks in agricultural decision-making. Meteorol. Appl. 13, 305–315.